



# Case Study of $^{137}\text{Cs}$ : Optimizing Counting Conditions with Different Background Region Width Selection

Ilker Can Celik<sup>1\*</sup>, Kadir Dagli<sup>2</sup>

<sup>1\*</sup> Harran University, Faculty of Art and Science, Department of Physics, Sanlıurfa, Turkey, (ORCID: 0000-0002-2320-6584), ilkercan0066@harran.edu.tr  
<sup>2</sup> Harran University, Faculty of Art and Science, Department of Physics, Sanlıurfa, Turkey, (ORCID: 0000-0001-5871-3159), 195105005@ogrenci.harran.edu.tr

(1st International Conference on Applied Engineering and Applied Natural Sciences ICAENS 2022, May 10-13, 2022)

(DOI: 10.31590/ejosat.1007743)

**ATIF/REFERENCE:** Celik, I. C. & Dagli, K. (2022). Case Study of  $^{137}\text{Cs}$ : Optimizing Counting Conditions with Different Background Region Width Selection. *European Journal of Science and Technology*, (36), 168-174.

## Abstract

Throughout the years, an optimizing counting conditions and optimum background region width determination has been carried out by several methods in gamma-ray spectroscopy. The effect of various background region widths has been the focus on digital integration methods in photopeak analysis. As an application tool of this in nuclear physics, radioactive sources has been mostly used by the lower or the higher resolution detectors; such as NaI(Tl) or HPGe gamma-ray detectors. This resolution factor influences the distinguishability of the peaks in close proximity in spectra. Therefore, a new computational and statistical approach should be implemented to decrease the error factors contributed by one of each bin content, namely the counts, in gamma-ray spectra. At this point, greater precision might be needed and reached in testing different bin region widths on each side of the range of interest for an individual peak. In specific, Gilmore's Total Peak Area (TPA) method will be used here to measure and analyze the background region width comparisons and their effects in the precision of counting gamma-rays by a NaI(Tl) scintillation detector.

**Keywords:** Gamma-ray spectroscopy, photopeak, digital integration methods, TPA method, background counting

## Farklı Taban Sayımı Genişliği Seçimleriyle Sayım Sayısı Optimizasyonunun $^{137}\text{Cs}$ Örneği

### Öz

Yıllar boyunca, sayım koşullarının ve taban sayımı bölgesi genişliğinin optimizasyonunun belirlenmesi gama spektroskopisinde birçok yöntem vasıtasıyla araştırılmıştır. Fotopik analizindeki dijital entegrasyon yöntemleri içinde, taban sayımı bölgesinin genişliğinin çeşitli etkileri halen odak noktası olmayı sürdürmektedir. Bu araştırmanın nükleer fizikteki uygulama aracı, çoğunlukla gama ışını algılamada kullanılan NaI(Tl) ve HPGe detektörleri gibi düşük veya yüksek çözünürlüklü detektörlerle algılanan radyoaktif kaynaklar olmuştur. Çözünürlükten kaynaklanan bu faktör, spektrumlarda çok iç içe bulunan piklerin ayırt edilmesine etki etmektedir. Bu yüzden, gama spektroskopisinde, her bir kanaldaki sayım sayısından gelebilecek hata paylarını azaltmak için bilgisayar ve istatistiksel tabanlı yeni yöntemler uygulanmalıdır. Bu noktada, her bir pik için farklı bin (kanal) bölgesi genişlikleri kullanılıp test edilerek daha iyi netlikte sonuçlar elde edilebilir. Bu çalışmada spesifik olarak NaI(Tl) sintilasyon detektörü kullanılarak, Gilmore'un Toplam Pik Alanı (TPA) metoduyla farklı taban sayımı bölgesi genişliklerinin sayım sayısı ölçüm duyarlılığı ölçülüp analiz edilecektir.

**Anahtar Kelimeler:** Gama ışını spektroskopisi, fotopik, dijital entegrasyon yöntemleri, TPA metodu, taban sayımı.

\* Corresponding Author: [ilkercan0066@harran.edu.tr](mailto:ilkercan0066@harran.edu.tr)

# 1. Introduction

In this work, optimum background region width identification will be investigated as one of the gamma-ray counting optimizing conditions. Gilmore's version of TPA method [2] has been chosen for the best suited tool for the analysis. Other numeric analysis approaches stated in the articles [3-11] has pros and cons in terms of analysing the digital data from a multichannel analyser (MCA) on gamma-ray absorption peaks in gamma-ray spectroscopy. The reason why the method in the article will be implemented is that it gives flexibility on where and how many of the channels (bins) can be selected in the peak region of interest. It will be explained in detail in following parts. When it comes to a data, radioactive <sup>137</sup>Cs point source provides the one clean individual photopeak at 661.7 keV energy and nothing else in the neighbouring region. Total channel number of 1024 has been used to collect the data. The corresponding peak falls around the channel number between 222 and 272. In a spectrum with bin width 1, the data indicates almost flat background on the left in the channel number range of 185-222 and on the right starting from channel number 272 onwards. The rest of the regions are out of interest for this work. Uncalibrated data showing the channel versus counts in Fig. 1 can be seen for the record. Most of the characteristics of a gamma-ray spectroscopy is also visible which makes the analysis much convenient than other complicated ones.

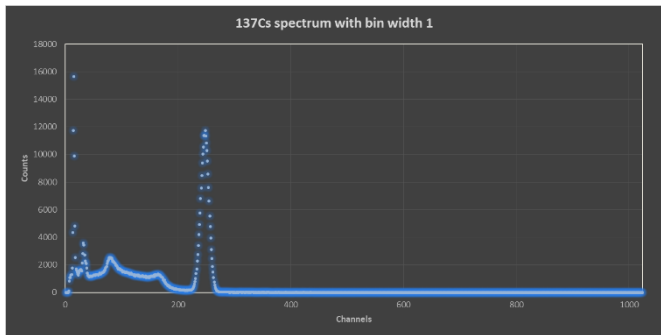


Figure 1: Spectrum of a radioactive <sup>137</sup>Cs point source.

For the purpose of the work, there should not be any other adjacent peaks with overlapping regions. As Figure 2 indicates, <sup>137</sup>Cs goes 100% Beta minus decay process to different levels

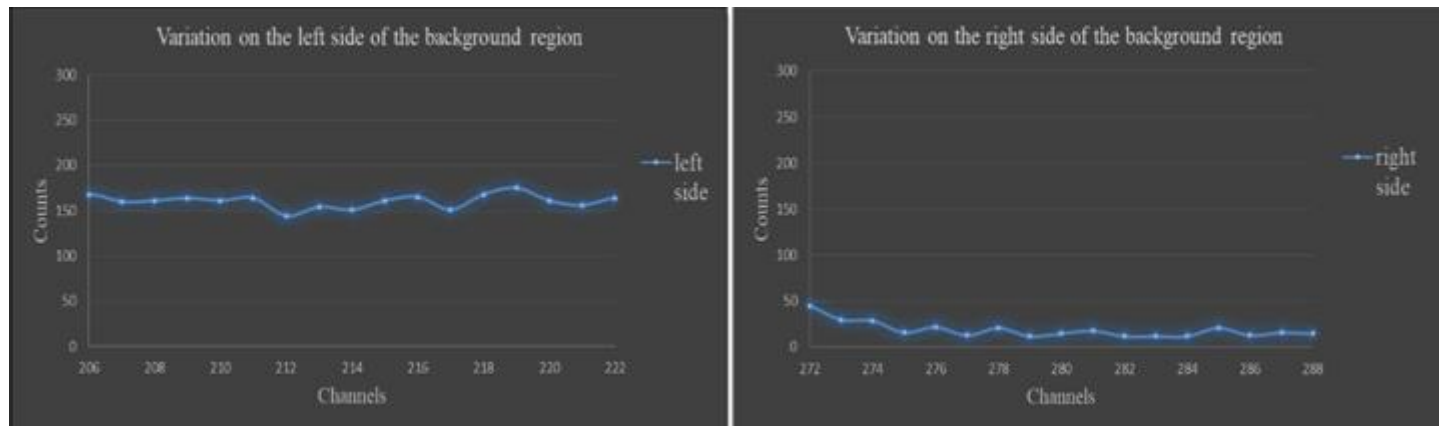


Figure 3: Statistical count variations in background region of 661.7 keV peak in <sup>137</sup>Cs on both side of the photpeak.

of <sup>137</sup>Ba nucleus. What's seen in the Fig. 1 is the strongest photopeak going directly to the ground state of

<sup>137</sup>Ba. To adjust and identify the optimum background region width, analyst should look on both side of the region of interest where the peak is located.

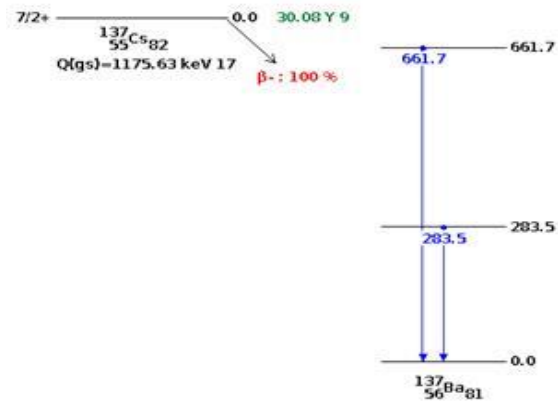


Figure 2: Decay scheme of radioactive <sup>137</sup>Cs source [1].

Figure 3 clearly states that the pattern in count change on both side of the peak region is almost stable. Fluctuations are ignorable. Also, the declining shape of the background is obvious by showing the count drop from 160s to 20s in average. One of the most challenging modellings in gamma-spectroscopy to estimate the background area under a peak is to choose the right representation of this falling pattern. For the rest of the section, the numerical approach and the optimization details will take place.

# 2. Methods and Conclusions

What Gilmore [2] suggested in his equations, written down below, was that the channel selection for the estimation of background counts cannot be fixed by the software and the analysts. They should have adjustable amounts in terms of specific layout position of the photopeak within the spectrum

$$A = \sum_{i=L}^U a_i - [(U - L + 1) \times \frac{(\sum_{i=L-m_L}^{L-1} a_i + \sum_{i=U+1}^{U+m_U} a_i)}{(m_L + m_U)}] \quad (1)$$

The variance can be indicated as below:

$$Var(A) = \sum_{i=L}^U a_i + [(\frac{U-L+1}{m_L+m_U})^2 \times (\sum_{i=L-m_L}^{L-1} a_i + \sum_{i=U+1}^{U+m_U} a_i)] \quad (2)$$

While the first equation emphasizes the effect of the background count on a net count denoted as A, the second equation indicates the weight of the background region width in the sum to calculate the variance. Every addition channel put in to this sum will contribute to the precision of the net area in turn. However, as more channels are added, there will be decreasing returns. The possibility of adjacent peaks must not be missed out because the wider the peaks and the background regions are, the more the deviation from linearity is in the background estimation models for analytic solutions. Here, the right question to ask is what the optimum number of channel must be. This clearly depends upon the circumstances as said earlier.

Figure 3 zooms into the region of interest on both side of the peak mentioned in the Fig. 1. While the fluctuation on the left side tanges between the counts of 144 and 175, it lays between 12 and 45 on right side of the photopeak. Note that these limits has been started right on the edge of the limits of the selected peak area. Figures 3-6 represents the real <sup>137</sup>Cs data and its peak region around 661.7 keV taken from an actual gamma-ray spectrum as a function of the width of the background region. The uncertainty on the peak area estimate is expressed as percentage relative standard deviation (RSD) in Figures 4-7. It is apparent that RSD decreases as the number of channels used to estimate the background increases. When two channels indicates obviously considerable improvement on one, the selection of three channels is rather better than two are. However, the reduction in uncertainty with each extra channel used shows smaller and smaller pattern throughout the analysis. This concludes that there will be a little extra value in using more than three or four channels.

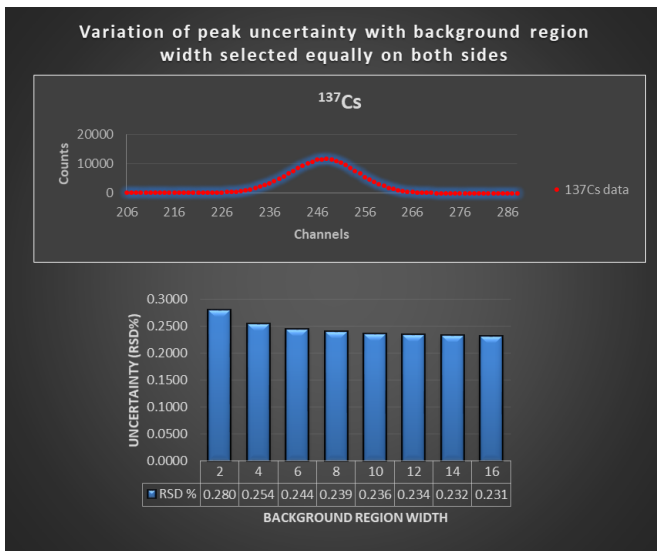


Figure 4: Variation of peak area uncertainty in RSD on each sides of the selected peak at 661.7 keV in actual <sup>137</sup>Cs source.

Even in practice, the presence of neighbouring peaks may automatically limit the width of the background region into very strict area. It's again the most important thing in the analysis that analyst should investigate every situation individually.

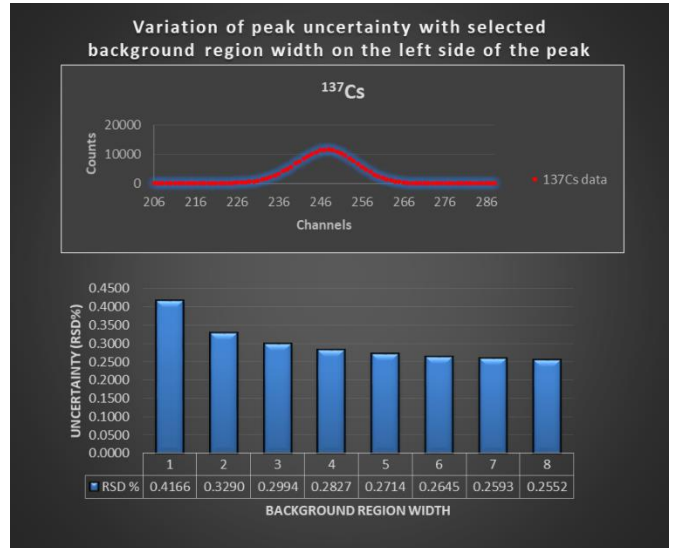


Figure 5: Variation of peak area uncertainty in RSD on the left side of the selected peak at 661.7 keV in actual <sup>137</sup>Cs source.

If the peak is well defined as in the case of <sup>137</sup>Cs in comparison to ill-defined, then there may be little to be gained by using more than three or four channels. In such cases, the background uncertainty will have a much smaller effect on the uncertainty of the net peak area estimate as they will be shown in Table 1-3. Note that the number of channels used for background estimate does not show any statistically substantial effect on the net area. Despite that, it gives drastically varying values in the background errors.

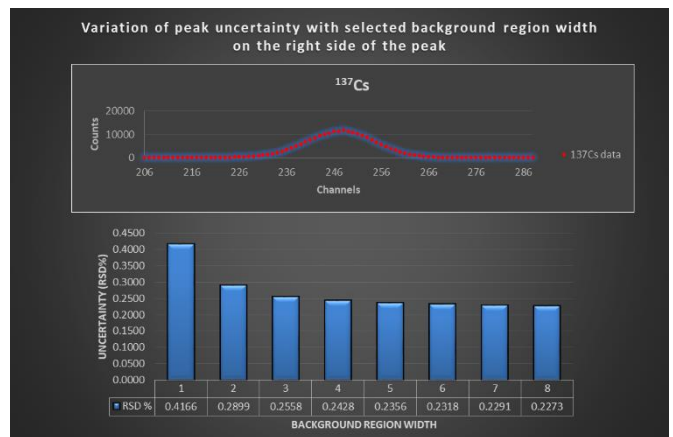


Figure 6: Variation of peak area uncertainty in RSD on the right side of the selected peak at 661.7 keV in actual <sup>137</sup>Cs source.

Another point in terms of digital softwares; such as Maestro and Scintivision, they have automatic spectrum analysis system where a compromise is usually made. In these commercial MCA and spectrum analysis programs, 3, 4 or 5 channels are usually used for the background calculations depending upon the manufacturer and the user. The fact here is that there is no fundamental reason why the width of the background region should be the same on both side of the peak region. If there were a potentially interfering neighbour above the peak, it would be sensible to use, say, even one or two channels above and, perhaps, more in the below side. In such a case, the term  $m_L + m_U$  is used, where  $m_L$  and  $m_U$  are the lower and upper background region widths.

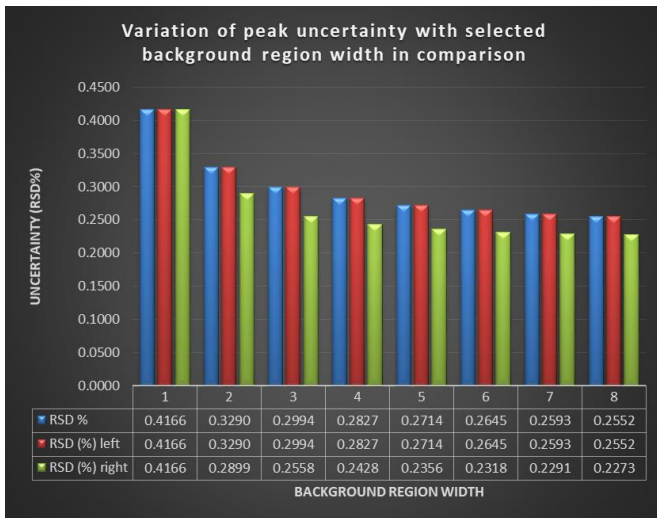


Figure 7: Comparisons in variations of the peak area uncertainty as RSD with a comparison table among the three conditions mentioned in the Figures 4-6.

The selection of these widths is up to the analyst. This choice can be easily made independently, depending upon whether the background has a flat pattern for the background continuum. In the first equation, first sum ( $\sum_{i=L}^U a_i$ ) gives the total count under the peak in a selected lower and upper range. Therefore, this

value will remain the same in all tables as long as lower limit (L) and upper limit (U) are fixed. However, the second part in the first equation gives the deduction of the background part. It calculates the background count by multiplying the total channel number with the average value of the counts within the channels of  $m_L$  and  $m_U$ . Everytime  $m_L$  and  $m_U$  parameters change, the results for the total background counts and its variance will change. These results can be compared also when the background region side changes in the Tables 1-3.

In the Table 2, the RSD values for one and two channels seem giving higher outcomes in comparison to the more channel selections. As the channel number gets higher, the net count errors tend to be stabilized. The same situation happens just after the first channel in the background region width in the Table 3. As a summary, the decreasing trend on RSD values in all tables has consistency among each other regardless of the background region selection.

### 3. Acknowledgement

I'd like to thank to my master student Kadir Dağlı for his encouraging comments for the last three years. Also, I'd like to give my gratitude to the CERN's ROOT forum team for enlightening discussions.

Table 1: The results indicate the variations in background counts and its effect on the net counts under a selected photopeak at 661.7 keV energy in the case of  $^{137}\text{Cs}$  spectrum. The background range is chosen on both side of the peak as shown in  $m_L$  and  $m_U$  values as explained in the text below.

When background width selection region made on both side of the peak equally								
$m_L$	1	2	3	4	5	6	7	8
$m_U$	1	2	3	4	5	6	7	8
Background region width	2	4	6	8	10	12	14	16
L- $m_L$	221	220	219	218	217	216	215	214
L-1	221	221	221	221	221	221	221	221
L	222	222	222	222	222	222	222	222
U	272	272	272	272	272	272	272	272
U+1	273	273	273	273	273	273	273	273
U+ $m_U$	273	274	275	276	277	278	279	280
$n=U-L+1$	51	51	51	51	51	51	51	51
$a_0$	247	247	247	247	247	247	247	247
Gross area	209336	209336	209336	209336	209336	209336	209336	209336
variance	209336	209336	209336	209336	209336	209336	209336	209336

error	458	458	458	458	458	458	458	458
Background area	4743	4794	4820	4826	4697	4705	4663	4609
variance	120947	61124	40966	30765	23955	19995	16986	14692
error	348	247	202	175	155	141	130	121
Net area	204593	204542	204517	204510	204639	204631	204673	204727
variance	330283	270460	250302	240101	233291	229331	226322	224028
error	575	520	500	490	483	479	476	473
uncertainty (RSD%)	0.2809	0.2543	0.2446	0.2396	0.2360	0.2340	0.2324	0.2312

Table 2: The results indicate the variations in background counts and its effect on the net counts under a selected photopeak at 661.7 keV energy in the case of <sup>137</sup>Cs spectrum. The background range is chosen on the left side of the peak as shown in m<sub>L</sub> and m<sub>U</sub> values as explained in the text below.

When background width selection region made on the left side of the peak								
m <sub>L</sub>	1	2	3	4	5	6	7	8
m <sub>U</sub>	0	0	0	0	0	0	0	0
Background region width	1	2	3	4	5	6	7	8
L-m <sub>L</sub>	221	220	219	218	217	216	215	214
L-1	221	221	221	221	221	221	221	221
L	222	222	222	222	222	222	222	222
U	272	272	272	272	272	272	272	272
U+1	273	273	273	273	273	273	273	273
U+m <sub>U</sub>	273	273	273	273	273	273	273	273
n=U-L+1	51	51	51	51	51	51	51	51
a <sub>0</sub>	247	247	247	247	247	247	247	247
Gross area	209336	209336	209336	209336	209336	209336	209336	209336
variance	209336	209336	209336	209336	209336	209336	209336	209336
error	458	458	458	458	458	458	458	458
Background area	9486	8849	8874	8798	8578	8551	8502	8402

variance	483786	225637	150858	112168	87498	72684	61946	53564
error	696	475	388	335	296	270	249	231
Net area	199850	200488	200462	200539	200758	200785	200834	200934
variance	693122	434973	360194	321504	296834	282020	271282	262900
error	833	660	600	567	545	531	521	513
uncertainty (RSD%)	0.4166	0.3290	0.2994	0.2827	0.2714	0.2645	0.2593	0.2552

Table 3: The results indicate the variations in background counts and its effect on the net counts under a selected photopeak at 661.7 keV energy in the case of <sup>137</sup>Cs spectrum. The background range is chosen on the right side of the peak as shown in m<sub>L</sub> and m<sub>U</sub> values as explained in the text below.

When background region width selection region made on the right side of the peak								
m <sub>L</sub>	0	0	0	0	0	0	0	0
m <sub>U</sub>	1	2	3	4	5	6	7	8
Background region width	1	2	3	4	5	6	7	8
L-m <sub>L</sub>	221	221	221	221	221	221	221	221
L-1	221	221	221	221	221	221	221	221
L	222	222	222	222	222	222	222	222
U	272	272	272	272	272	272	272	272
U+1	273	273	273	273	273	273	273	273
U+m <sub>U</sub>	273	274	275	276	277	278	279	280
n=U-L+1	51	51	51	51	51	51	51	51
a <sub>0</sub>	247	247	247	247	247	247	247	247
Gross area	209336	209336	209336	209336	209336	209336	209336	209336
variance	209336	209336	209336	209336	209336	209336	209336	209336
error	458	458	458	458	458	458	458	458
Background area	9486	5483	3927	3226	2713	2440	2178	2002
variance	483786	139804	66759	41128	27675	20736	15871	12761

error	696	374	258	203	166	144	126	113
Net area	199850	203854	205409	206110	206623	206897	207158	207334
variance	693122	349140	276095	250464	237011	230072	225207	222097
error	833	591	525	500	487	480	475	471
uncertainty (RSD%)	0.4166	0.2899	0.2558	0.2428	0.2356	0.2318	0.2291	0.2273

## References

1. Pritychenko, B. (17.04.2022). NNDC, Brookhaven National Laboratory. <https://www.nndc.bnl.gov/nudat3/NuDatBandPlotServlet?nucleus=137Ba&unc=nds>.
2. GILMORE, G.R.,2008.Practical Gamma Ray Spectrometry. John Wiley & Sons, Ltd,England,387s.
3. COVELL,D.F.,\_1959\_Determination of Gamma-Ray Abundance Directly from the Total Absorption Peak. Analytical Chemistry,31(11):1785-1790.
4. HEYDORN,K., LADA,W.,1972. Peak Boundary Selection in Photopeak Integration by the Method of Covell. Analytical Chemistry,44(14):2313-2317.
5. LOSKA,L.,1988. A modification of the “total peak area” (TPA) method for gamma ray spectra. Appl.Radiat.Isot.,39(6):475-477.
6. BAEDECKER,P.A..1971.Digital Methods of Photopeak Integration in Activation Analysis. Analytical Chemistry,43(3):405-410.
7. STERLINSKI, S.,1968. Analysis of digital data from a multichannel pulse height analyzer on gamma ray total absorption peaks. Analytical Chemistry,40(13):1995-1998.
8. KOKTA, L. 1973. Determination of peak area. Nuclear Instruments and Methods, 112:245-251.
9. BAEDECKER, P.A., GROSSMAN, J.N. 1989. The Computer Analysis of High Resolution Gamma-Ray Spectra from Instrumental Activation Analysis Experiments. Open-File Report:89-454. U.S. Geological Survey. DOI:10.3133/ofr89454.
10. A65-B32 Software’s User’s Manual. Ortec Part No. 777800. Available: <https://www.ortec-online.com/-/media/ametektortec/manuals/a65-mnl.pdf> [Access on: 1th September 2020].
11. KENNEDY,G.,1990. Comparison of photopeak integration methods. Nuclear Instruments and Methods in Physics Research A 299: 349-353.